A Journal of the Gesellschaft Deutscher Chemiker

Angewandte International Edition GDCh Chemie

www.angewandte.org

Accepted Article

Title: Macrodiolide Diversification Reveals Broad Immunosuppressive Activity That Impairs the cGAS-STING Pathway

Authors: Han Liu, Rasmus Ottosen, Kira Jennet, Esben Svenningsen, Tobias Kristensen, Mette Biltoft, Martin Roelsgaard Jakobsen, and Thomas Bjørnskov Poulsen

To be cited as: *Angew. Chem. Int. Ed.* 10.1002/anie.202105793

Link to VoR: https://doi.org/10.1002/anie.202105793

WILEY-VCH

10.1002/anie.202105793

Macrodiolide-diversification reveals broad immunosuppressive activity that impairs the cGAS-STING pathway

Han Liu[1,§,*], Rasmus N. Ottosen[1], Kira M. Jennet[1], Esben B. Svenningsen[1], Tobias F. Kristensen[1], Mette Biltoft[2], Martin R. Jakobsen[2,3,*], Thomas B. Poulsen[1,*]

[1] Department of Chemistry, Aarhus University, Langelandsgade 140, DK-8000, Aarhus C, Denmark.

[2] STipe Therapeutics ApS, c/o The Kitchen, Peter Sabroes Gade 7, DK-8000 Aarhus C, Denmark

[3] Department of Biomedicine, Aarhus University, Høegh-Guldbergs Gade 10, DK-8000, Aarhus C, Denmark

[§] Current address: Department of Chemistry, The University of Hong Kong, Pokfulam Road, Hong Kong SAR, P. R. China.

[*] e-mail: thpou@chem.au.dk, mrj@biomed.au.dk, liuhan@hku.hk

Abstract.

The development of new immunomodulatory agents can impact various areas of medicine. In particular, compounds with the ability to modulate innate immunological pathways hold significant unexplored potential. Here, we report a modular synthetic approach to the macrodiolide natural product (-)-vermiculine, an agent previously shown to possess diverse biological effects including cytotoxic and immunosuppressive activity. The synthesis allows for a very high degree of flexibility in introducing new modifications to the macrocyclic framework including the formation of all possible stereoisomers. In total 18 analogues were prepared. Biological characterization revealed that analogues LH531 and LH519, which both possess very minor structural modifications, had clearly enhanced cancer cell line selectivity and reduced toxicity. Moreover, these compounds possessed broad inhibitory activity against innate immunological pathways in human PBMCs, including the DNA-sensing cGAS-STING pathway. Initial mechanistic characterization suggests a surprising impairment on the STING-TBK1 interaction that prompts interesting questions for future studies of the immunosuppressive actions.

Key words.

Natural products; Total synthesis; Modular synthesis; Immunosuppressive agent; cGAS-STING

10.1002/anie.202105793

Introduction

Natural products and their derivatives play central roles in the arsenal of immunosuppressive agents for human medicine[1], spanning from the topical treatment of local skin inflammation and alleviation of autoimmune-diseases to the transplantation of vital organs. The immunosuppressive mechanisms used by known drugs target mainly the humoral or cell-based immune responses. Whereas glucocorticoids, such as hydrocortisone or its derivatives dexamethasone/prednisone, engage a plethora of pathways in both B- and T-cells[2], macrocyclic natural products, such as cyclosporin A and FK506, specifically target the activation of T-cells through blockade of calcineurin-dependent signalling[3]. Recently, dampening of hyper-inflammation related to infection with the pandemic respiratory virus SARS-CoV-2, has proven to be another important application of immunosuppressants.[4] In addition, pharmacological modulators of innate immune pathways are experiencing increasing interest, driven in large part by advances in immuno-oncology. The cGAS-STING pathway, in particular, has gained attention as it has been demonstrated to play a key function in various auto-immune diseases[5,6], including systemic lupus erythematosus (SLE)[7,8] and type I interferonopathies[9,10]. The involvement of immunologic responses in most disease settings, underscores the continued importance of development of immunomodulatory agents (suppressants as well as activators), including the re-investigation of agents previously identified to possess relevant activities. Here, we report studies which originate from such a compound, the natural product vermiculine.

Vermiculine (**1**, Figure 1A) was first isolated from *Penicillium vermiculatum* by Kuhr and co-workers in 1972,[11] and later re-isolated from *Talaromyces wortmannii*.[12] In preliminary biological tests, the compound showed weak antibacterial and antifungal activity and more potent anticancer and antiprotozoal activity.[11,13,14] Vermiculine was found to possess immunosuppressant activity against both human and murine cells[15,16,17] and the compound e.g. inhibited concanavalin A-stimulated cytokine production (IL-2, IL-4, IL-10, IFN-γ) in murine spleen cells and LPS/IFN-γ-stimulated NO production in macrophages.[17] The effects on *in vitro* cytokine production were, however, accompanied by an anti-proliferative effect with a relatively narrow selectivity window (<5 fold). A more detailed mapping of the specific pathways affected by vermiculine has not been performed. Interestingly, in an *in vivo* skin allograft survival experiment in mice, vermiculine (50 mg/kg) significantly improved the survival of the grafted tissue, and, furthermore, co-treatment with cyclosporin A (CsA) augmented this effect, underscoring the interesting immunosuppressive profile.[17] Furthermore, despite of the substantial anti-proliferative effects *in vitro*, the compound shows an apparent low systemic toxicity *in vivo* (intraperitoneal acute LD_{50} 420 mg/kg in mice)[11]. Structurally, vermiculine features two Michael acceptor-functionalities within the macrocycle (Figure 1A). Our lab has a sustained interest in unusual electrophiles[18,19,20,21,22] and in the present case, we wondered if the presence of these – presumably quite reactive – keto-enoate groups play a key role for the immunosuppressive activity and whether their structural manipulation would allow for improvement of the *in vitro* pharmacological profile.

Due to the insufficient availability of the compound from natural sources and limitations of current late-stage peripheral modification methods, a broad structure-activity study of vermiculine can only be facilitated by total synthesis. In recent years, even very complex scaffolds has been brought within the realm of traditional medicinal chemistry through diverted total synthesis.[23,24,25,26,27] By design of typically highly modular[28,29] synthetic routes, a whole family of natural products and analogues bearing multiple modifications can be achieved within a minimized number of steps to facilitate biological studies.[30,31] In addition, alternative synthesis paradigms that e.g. seek to fuse natural product building blocks through unnatural connections[32,33] or construct new complex scaffolds from abundant natural products[34,35] has also been developed to access natural-product-like chemical space. Being a modest-sized member of the C_2-symmetric macrodiolide family[36,37] vermiculine has attracted the attention of synthetic chemists, with the first (racemic) synthesis reported by Corey.[38] In total, three racemic and four asymmetric syntheses have been reported.[39,40,41,42,43,44,45] Most recently, Breit and co-workers used their Rh-catalyzed asymmetric dimerization of allenyl carboxylic acids,[46,47] to efficiently prepare the 16-membered macrodiolide core of

10.1002/anie.202105793

vermiculine, which could be further elaborated to the natural product in two additional steps.[45] Despite multiple inspiring transformations, these earlier target-directed approaches do not perfectly satisfy the demands required for a generalized approach to vermiculine-inspired C_2- and non-C_2-symmetric macrodiolides. Consequently, we set out to design a new two-phase synthesis towards vermiculine-inspired macrodiolides and report here the first results from these efforts along with the discovery of analogues with reduced toxicity that display inhibitory activity against innate immunological pathways, including the cGAS-STING pathway.

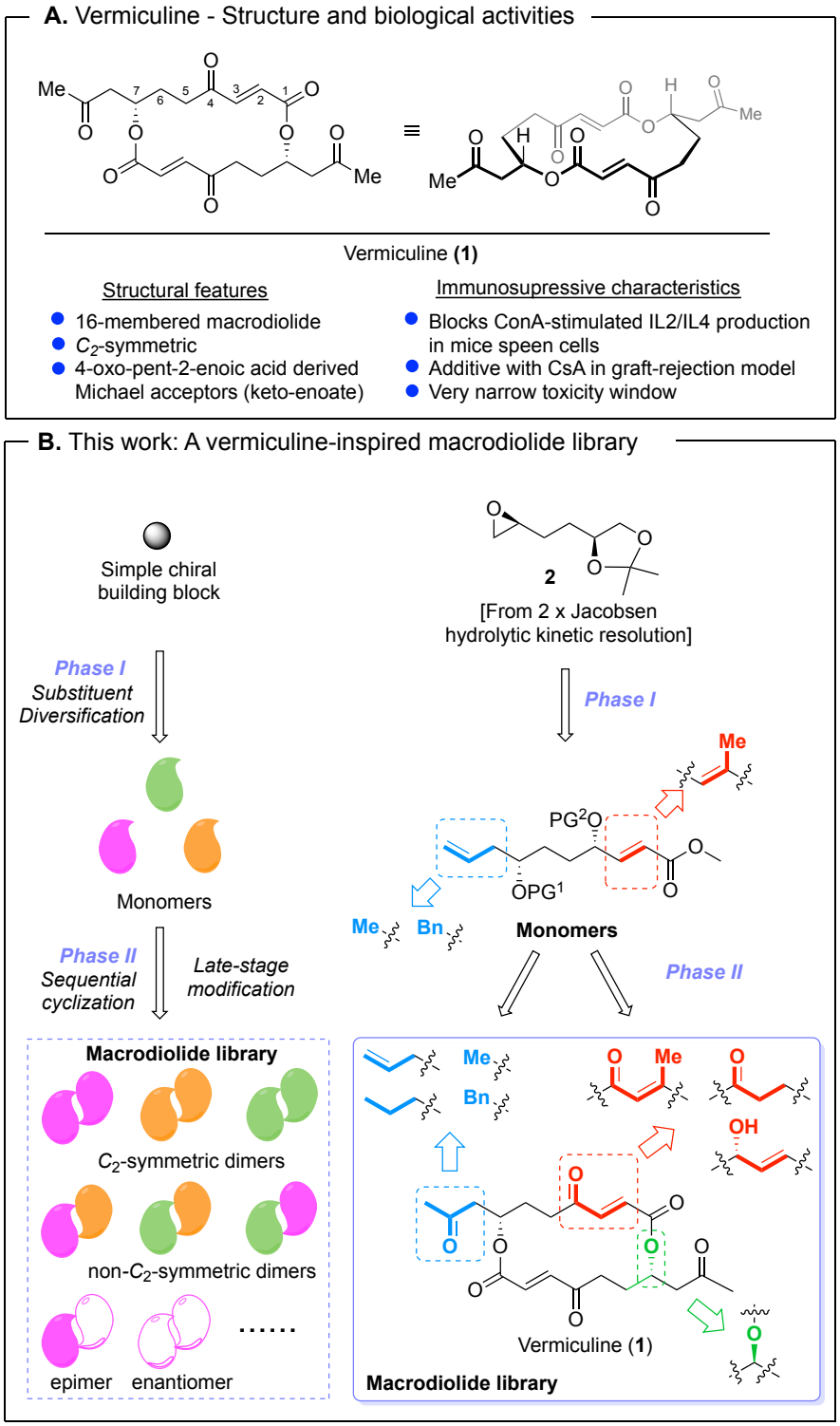

Figure 1. Structure and biological activities of vermiculine and the design of a two-phase synthesis to prepare a vermiculine-inspired macrodiolide compound collection.

10.1002/anie.202105793

Results and Discussion

Two phase synthesis of vermiculine

We sought to develop a synthetic approach (Figure 1B) that would start from a readily available common starting material to first prepare a series of structurally distinct monomers following similar transformations (phase I). Next, the final macrodiolide compounds, bearing variations on both halves, would be prepared via stepwise homo- and hetero-dimerization of the different monomers and subsequent tailoring modifications (phase II). In the case of vermiculine (Figure 1B), we identified chiral epoxide **2**,[48] which can be prepared via asymmetric kinetic resolution (Figure S1, Supporting Information), as an optimal starting material. In phase I, this building block allows for the flexible introduction of different substituents via nucleophilic opening of the terminal epoxide and for enoate formation using different Wittig reagents. In Phase II, the different monomers can be dimerized via esterification under either condensation or Mitsunobu conditions to achieve macrodiolide structures with both functional group and full stereochemical diversity.

As a representative example of this approach, our new route to vermiculine **1** is shown in Figure 2. The epoxide **2** was opened by vinylmagnesium bromide to afford homoallylic alcohol **3**. After acetonide removal, the resulting vicinal diol was converted to the 4-methoxybenzaldehyde acetal **4** and a *tert*-butyldimethyl silyl (TBS) group was installed at the C7-carbinol. After regioselective opening of the acetal by DIBAL-H at low temperature, orthogonally protected primary alcohol **5** was generated in 95% yield (66% total yield from **2**) accompanied by negligible amount of the regioisomer. The primary alcohol was oxidized by BAIB/TEMPO to give the crude aldehyde, which was directly submitted to the Wittig olefination to afford the *trans*-enoate **7** in 75% yield over two steps. The enoate **7** could then be divergently processed by treatment with either LiOH or Olah's reagent (HF/pyridine) to give the acid **8** and alcohol **9**, respectively. Very efficient ligation of the two monomers was possible using the Yamaguchi esterification to give linear dimer **10** in 95% yield. Other esterification conditions using PyBOP, HATU and DCC gave much inferior results in this transformation.[49] After selective hydrolysis of the less hindered methyl ester and TBS-group removal by Olah's reagent, the so-obtained seco-acid **11** was cyclized via Yamaguchi macrolactonization to give macrodiolide **13** in excellent (80%) yield. Next, we used the Wacker oxidation of both allyl groups to reveal the side chain ketone functionalities.[50] The optimized conditions utilized 0.4 equiv. of $PdCl_2$ and 0.4 equiv. of $Cu(OAc)_2$ under 1 atmosphere of O_2, while higher $Cu(OAc)_2$ loading led to oxidative deprotection of the PMB group. Still, due to the moderate branch/linear selectivity (~5:1), the bis-ketone product **14** was isolated in moderate 48% yield. Finally, vermiculine **1** was obtained in a high-yielding, two-step operation via oxidative removal of the PMB group and Dess-Martin oxidation of the released alcohol. The high flexibility and efficiency of this approach (9% overall yield, 14 steps in the longest linear sequence) satisfied our demand for library synthesis.

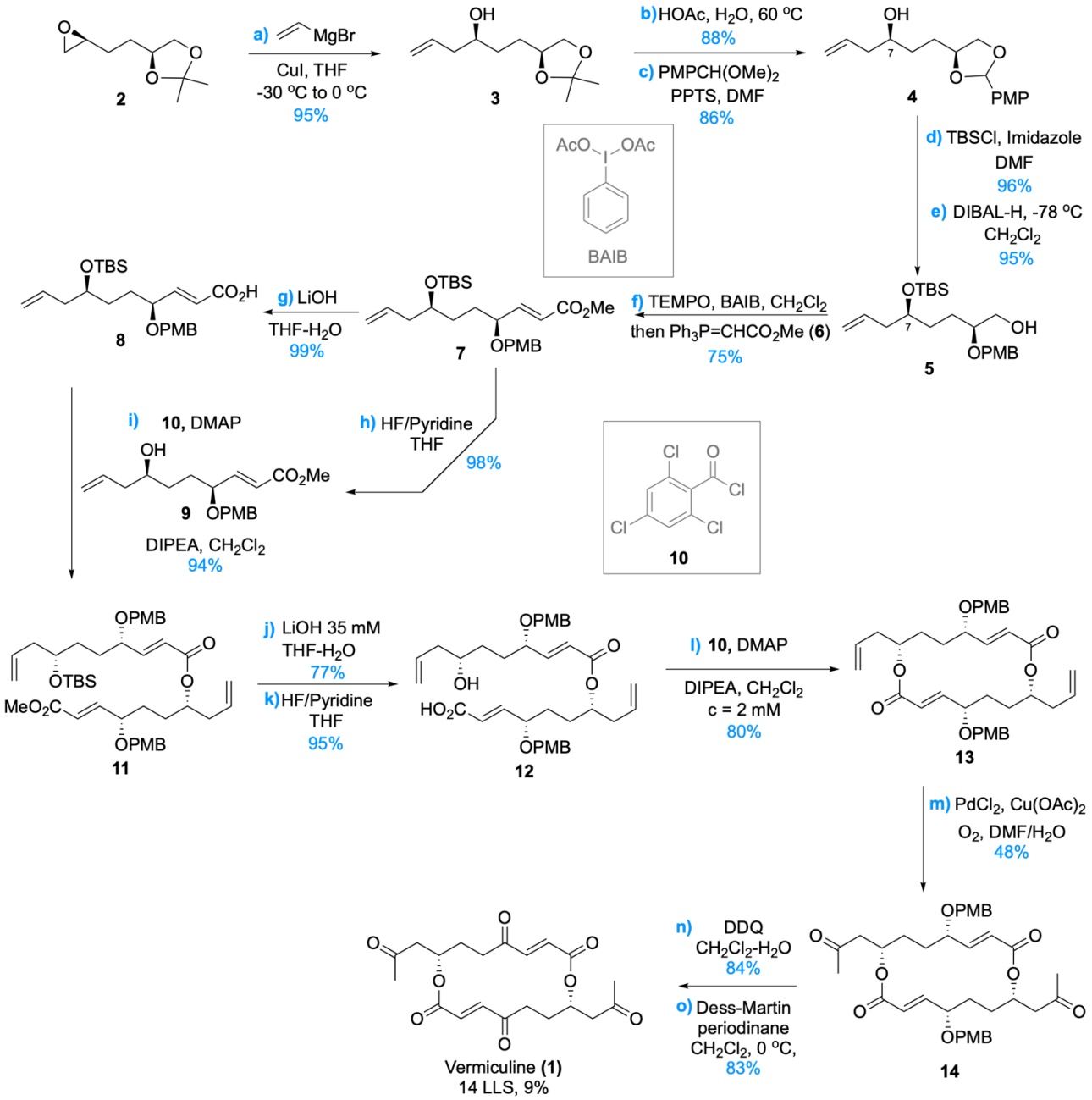

Figure 2. Total synthesis of vermiculine (**1**) from epoxide **2**. Abbreviations: THF = tetrahydrofuran, PMP = *para*-methoyphenyl, PPTS = pyridinium *para*-toluenesulfonate, DMF = *N,N*-dimethylformamide, TBS = *tert*-butyldimethylsilyl, DIBAL-H = diisobutylaluminium hydride, TEMPO = 2,2,6,6-Tetramethyl-1-piperidinyloxy, BAIB = Bis(acetoxy)iodobenzene, DIPEA = diisopropylethylamine, DMAP = *N,N*-dimethylaminopyridine, DDQ = 2,3-Dichloro-5,6-dicyano-1,4-benzoquinone.

Preparation of a focused library of vermiculine-related macrodiolides

Starting from the same epoxide **2**, we next targeted a collection of vermiculine analogs. As summarized in Figure 3 (see Supporting Information for complete details), we carried out the first epoxide ring-opening by DIBAL-H and vinyl/phenyl Grignard reagents and performed olefination using two different Wittig reagents. This afforded enoate monomers **7** and **15**-**17**. In the next phase, from macrodiolide **13** and Wacker oxidation product **14**, four analogs bearing allyl/propyl side chains (**18**-**21**) and two analogs bearing ketone side chains (**22**-**23**) were prepared respectively. From the same intermediate **7**, by using Mitsunobu reaction once or twice in the ester bond forming steps, the macrodiolides **24** and **28** with one or two

10.1002/anie.202105793

configurationally inverted chiral centers were prepared. Subsequently, enantiomer analogs **25**-**27** and epimer analogues **29**-**30** were prepared.

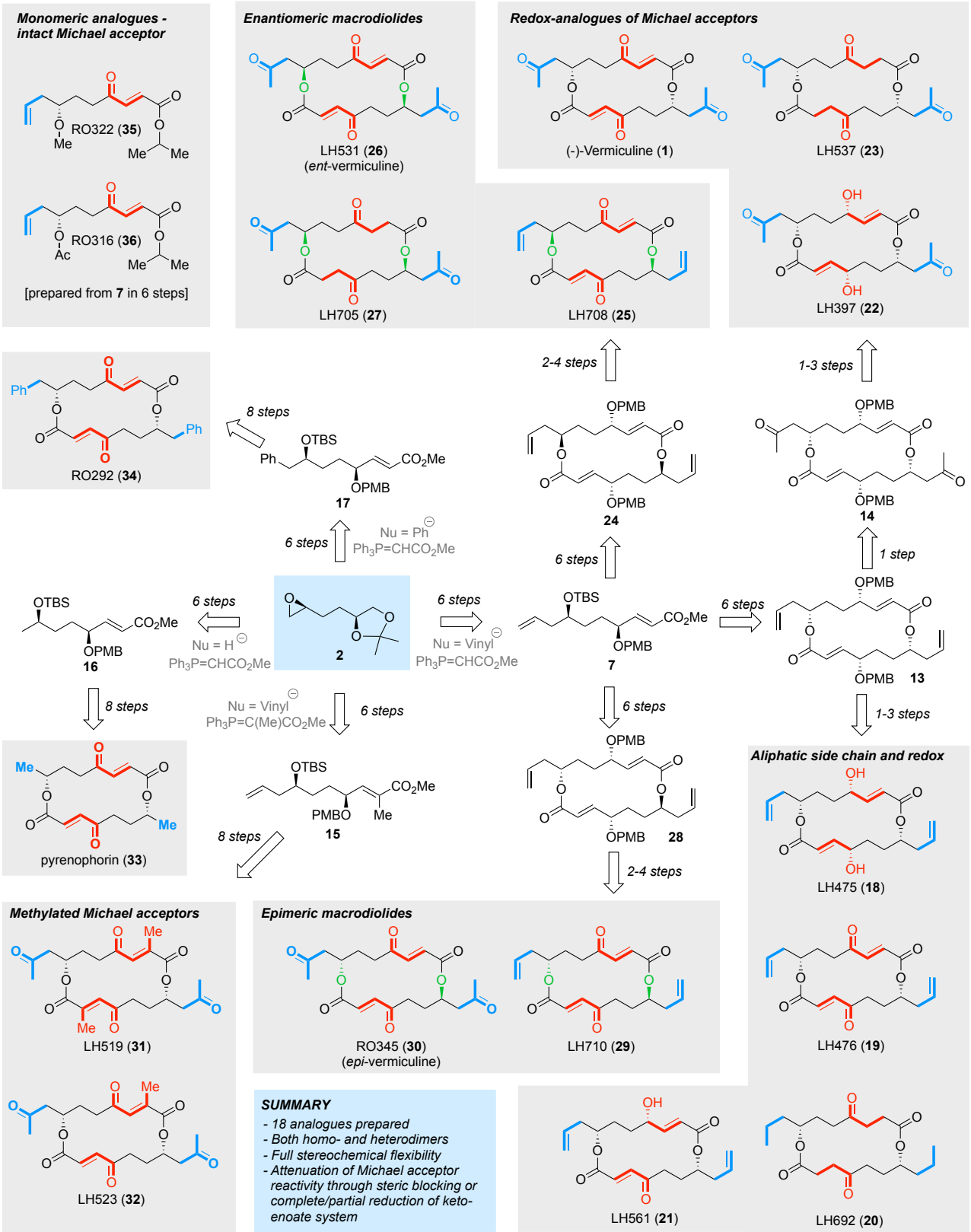

Figure 3. Preparation of vermiculine-related macrodiolides. Overview of the complete collection of compounds. See Supporting Information for details on the syntheses.

To investigate the relationship between the reactivity of the electrophilic keto-enoate moiety and the biological activity, C_2-symmetric analogue **31,** with both alkenes sterically blocked by methyl substituents,

and the corresponding non-C_2-symmetric compound **32** were synthesized from monomer **15**. Finally, to initially evaluate the effect of the side chain, vermiculine analogues **33** (known as pyrenophorin)[51] and **34** bearing methyl and benzyl side chains were prepared from monomers **16** and **17** respectively.

Cytotoxic activities of macrodiolide-analogs

With a sizable collection of compounds in hand for biological characterization, we initially performed a survey of the growth-inhibitory activities of the compounds across four different cancer cell lines (U-2OS, PC-3, MOLT-4, THP-1). These experiments might expose analogues with enhanced selectivity for specific cell lines and/or identify compounds with favorable toxicity profiles for further follow-up (Table 1 and Table S1). These experiments confirmed the significant growth-inhibitory activity for (-)-vermiculine (**1**) having an average IC_{50} of 5.1 μM with a relatively narrow span of IC_{50} (5.6-fold) across the four cell lines (entry 1). A related activity-pattern was observed for a series of different compounds (entries 4-12) all having intact Michael acceptor systems, possibly reflecting pleiotropic effects. On the contrary, compounds in which either both of the C4/C4'-ketones or the double bonds were reduced were nearly devoid of activity in this experiment (entries 14-18). Three compounds from the collection, however, stood out by displaying a significantly reduced level of activity in the monocyte/macrophage THP-1 cells: LH531 (**26**) and RO345 (**30**) being the enantiomer and epimer of vermiculine (entries 2-3), respectively, and LH519 (**31**) having two methyl groups positioned on the Michael acceptor system (entry 13). Interestingly, LH519 also had low activity in the U-2OS and PC-3 cells (IC_{50} >30 μM) but maintained potency in MOLT-4 cells (IC_{50} = 4.5 μM).

Table 1. Cell viability data for four cancer cell lines treated with macrodiolide analogs[a]

entry	electrophilic motif	Compound	U-2OS	PC-3	MOLT-4	THP-1	Average potency (μM)	Span
1	2X keto-enoate electrophile	(-)-Vermiculine (**1**)	4.1	7.3	1.8	7.4	5.1	5.6
2		LH531 (**26**)	4.9	5.3	1.2	39.3	13	38
3		RO345 (**30**)	3.4	8.6	1.9	33.9	12	32
4		LH476 (**19**)	1.4	2.1	1	6.3	2.7	5.3
5		Pyrenophorin (**33**)	2.1	2.2	0.7	7.8	3.2	7.2
6		RO292 (**34**)	0.7	1.6	0.7	4.1	1.8	3.4
7		LH708 (**25**)	0.4	1.2	0.4	6	2	5.6
8		LH710 (**29**)	0.6	1.3	0.4	5.8	2	5.4
9	1X keto-enoate electrophile	LH561 (**21**)	1.4	1.6	0.7	6.9	2.6	6.2
10		RO322 (**35**)	3	5.4	1.6	6.6	4.1	5
11		RO316 (**36**)	2.7	4.9	2.2	10.4	5	8.2
12		LH523 (**32**)	2.4	4.3	0.6	7.2	3.6	6.5
13	Attenuated	LH519 (**31**)	32.1	40	4.5	19.3	24	35.6
14		LH397 (**22**)	>50	>50	>50	>50	>50	nd
15		LH475 (**18**)	>50	>50	31.2	>50	>46	>18
16	reduced	LH537 (**23**)	>50	>50	>50	>50	>50	nd
17		LH705 (**27**)	7.9	22.5	>50	>50	>33	>42
18		LH692 (**20**)	36.5	>50	22.4	>50	>40	>28

[a] For the complete data set, including standard deviations, see Table S1 (Supporting Information). IC_{50} determinations are average of at least 3 independent biological replicates, each performed in technical triplicates. Color-coding, average potency (IC_{50}): <10 μM = green; 10-20 μM = yellow, 20-40 μM = orange; >40 μM = red; span (difference in IC_{50} between most sensitive and least sensitive cell line): <10 = green; 10-20 = yellow; 20-40 = orange; >40 = red.

Immunosuppressive activities of synthetic macrodiolide analogs

Next, we performed further evaluation of selected compounds as potential modulators of different and broad innate immune-signaling pathways; including cGAS-STING (doublestranded (ds) DNA sensing)[52], the RIG-I/TLR3 (RNA sensing)[53,54,55] and TLR4 (LPS sensing)[56]. We used human peripheral blood mononuclear cells (PBMCs) as all three signaling pathways are highly active in such heterogenous cell populations. Due to their reduced toxicity (Table 1), we selected LH531 (**26**) and LH519 (**31**) for these experiments and the non-toxic analog LH397 (**22**) was included as a control. In two different PBMC donors, we stimulated cells with either dsDNA/cGAMP (targeting cGAS-STING), PolyI:C (targeting RIG-I/TLR3) or soluble LPS (targeting TLR4) and subsequently measured the innate immunological activity through the production of type I Interferon (reporter bioassay) or pro-inflammatory cytokine production (hCXCL10 and TNF-α) 20 hrs post stimulation (Figure S2, Supporting Information). Interestingly, we found that both LH519 and LH531 (test concentration 3 μM) afforded a broad inhibitory activity against all tested stimuli (Figure S2). The very potent, near complete, inhibition observed with LH531 was accompanied by a loss of cell viability (ca. 25% of control in both donors), but LH519 did not afford any significant loss of cell viability (<10%). LH397 did not display any inhibitory effects (Figure S2). Prompted by the anti-cancer activity displayed by the compounds (Table 1), we decided to focus our next experiments on the cGAS-STING pathway. Using four additional PBMC donors, we next studied the dose-dependent inhibition of hCXCL10 production in response to dsDNA (Figure 4A and Figure S2) and found that LH531 elicit resolute inhibition of hCXCL10 in the lower micromolar range for all tested donors (Figure S2). In comparison, LH519 elicit a less potent inhibition of the cytokine response, nevertheless a complete inhibition of CXCL10 at high concentration (10μM) was generally observed. Importantly, at the highest drug concentration tested LH519 treatment had only minimal effects on cell viability (Figure 4A and Figure S2).

It is known that STING upon activation by the cyclic di-nucleotide 2'3'-cGAMP undergoes phosphorylation by the kinase TBK1, which triggers trans-phosphorylation of TBK1 and subsequently phosphorylation of STING at serine position 366. In the attempt to pinpoint signaling inhibition elicited by LH531 and LH519 on the dsDNA-STING-TBK1 axis, we next used a well-controlled model consisting of PMA-differentiated THP-1 cells. First, we confirmed that LH519 and LH531 were able to inhibit dsDNA-induced hCXCL10 production in this cell line (Figure 4B). We observed similar inhibitory patterns as seen in PBMCs, however a general higher concentration of compounds was needed, but without affecting cell viability, consistent with earlier data (Table 1). We then used immunoblotting to assess the degree of phosphorylation of STING and TBK1 upon treatment with LH519 and LH531 respectively. Interestingly, we observed that both compounds had the ability to block phosphorylation of STING at early timepoints, and at later timepoints LH531 demonstrated consistent inhibition of STING phosphorylation (Figure 4C). Counterintuitively, both compounds, especially LH531, let to increased phosphorylation of TBK1 (Figure 4C). To explore if the compounds were able to increase phosphorylation of TBK1 independent of a STING agonist we repeated the experiment at 4 hours stimulation and compared untreated and dsDNA treated cells. We confirmed that both LH519 and HL531 impaired STING phosphorylation, but rather unexpectedly we observed that LH531 resulted in a hyperphosphorylation of TBK1 independent of STING activation (Figure 4D). This suggests that the compound may either activate other intracellular kinases or induce TBK1 trans-phosphorylation but future studies will be needed to address this. Evaluating CXCL10 and type I IFN

responses at 20 hrs post stimulation confirmed that an early impairment of STING phosphorylation supported a clear drop in cytokine production (data not shown).

Collectively, our data suggests that vermiculine analogues LH519 and LH531 have broad suppressive activity of central signaling pathways of the innate immune response and specifically affect the STING pathway (Figure 4E). The keto enoate Michael acceptor functionalities appear to be required for the immunosuppressive activities of these compounds as e.g. the saturated analogue LH537 (similar to LH397) showed no ability to block dsDNA-stimulated CXCL10 production (Figure S2). Our data suggest that LH519, with its partially blocked Michael acceptor substructures, has an enhanced selectivity window and appears to be particularly interesting for follow-up studies due to its low toxicity.

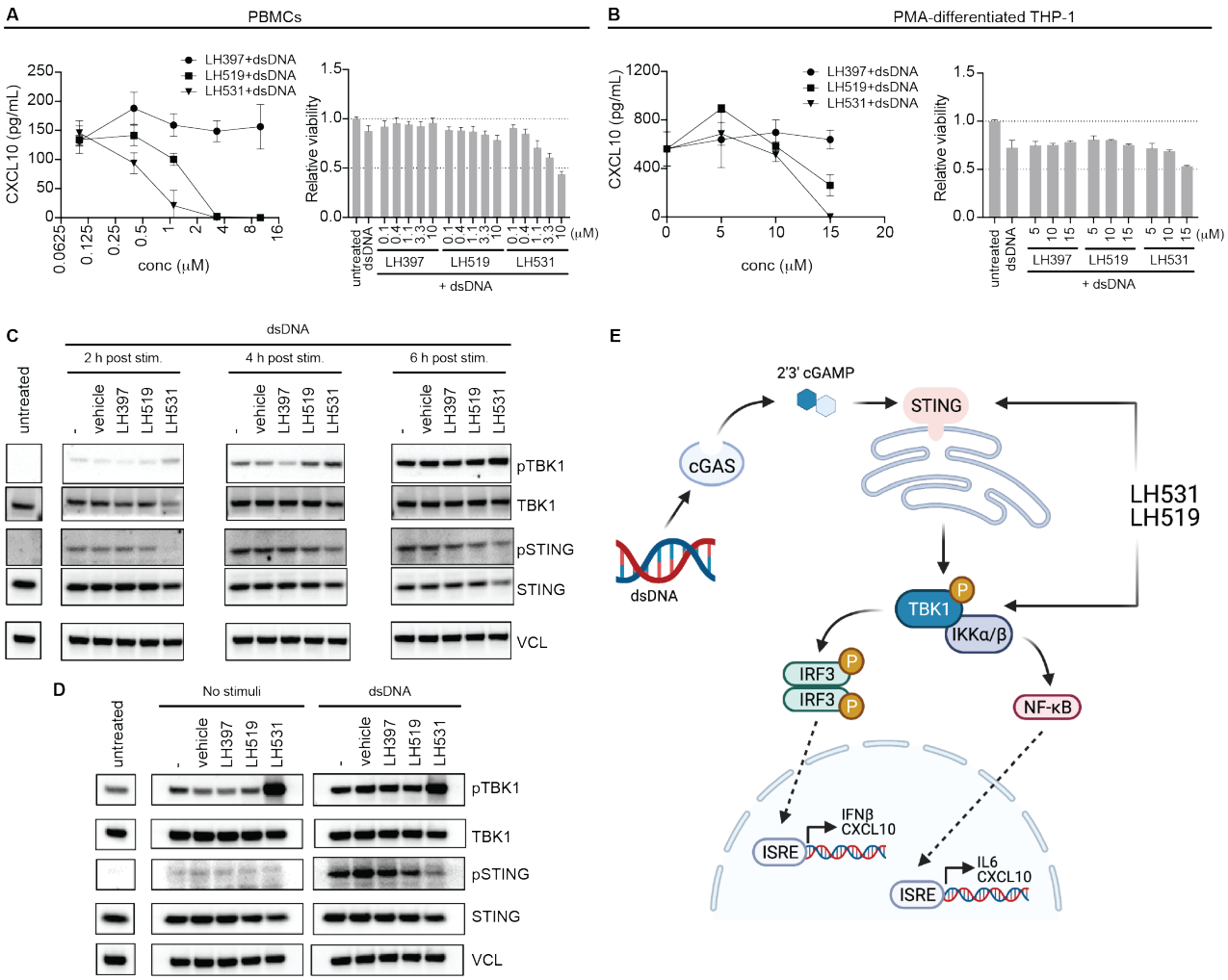

Figure 4. Inhibitory effects of macrodiolide analogs on the cGAS-STING pathway. **(A)** Human PBMCs and **(B)** PMA-differentiated THP-1 cells were primed with LH397, LH519, or LH531 for one hour and subsequently stimulated with dsDNA (1μg/mL). Twenty hours post dsDNA stimulation, supernatants were evaluated for CXCL10 protein expression and cell viability were analyzed by Celltiter Glo. **(C)** PMA-differentiated THP-1 cells were primed with LH397, LH519, or LH531 (15μM) for one hour and subsequently stimulated with dsDNA (1μg/mL). Two, four, and six hours post stimulations, cells were lyzed and protein expression and phosphorylation levels were evaluated by immunoblotting. **(D)** PMA-differentiated THP-1 cells were primed with LH397, LH519, or LH531 (15μM) for one hour and subsequently stimulated with dsDNA (1μg/mL) or left untreated. Four hours post stimulations, cells were lysed and protein expression and phosphorylation levels were evaluated by immunoblotting. **(E)** Illustration of the effect of macrodiolide analogs on the STING pathway. Data in (A) and (B) represent mean ± s.d. of biological triplicates.

Conclusion

In conclusion, we have developed a very efficient, yet highly flexible, diversity-focused synthesis of the macrodiolide natural product vermiculine and we have demonstrated its use for preparation of 18 different analogs. The synthesis constitutes a platform that will enable bespoke modifications to be introduced to this interesting macrocyclic scaffold. Biological evaluation revealed synthetic analogs that display both selective anti-cancer activity against MOLT-4 leukemia cells and inhibition of innate immune-signaling pathways of high current attention, including the cGAS-STING pathway. Our future efforts are focused on the inhibitory mechanism used by LH519 and LH531.

Acknowledgements

Financial support from the Novo Nordisk Foundation (grant NNF19OC0054782 to T.B.P.), the Carlsberg Foundation (grant CF17-0800 to T. B. P.) and Lundbeck Foundation (R238-2016-2708 to M.R.J.) is gratefully acknowledged.

Conflict of interest

MB and MRJ are both employees and shareholders of STipe Therapeutics, a biotech company focusing on targeting the STING pathway for cancer and immunological diseases. The remaining authors declare no competing interests

References

[1] Wiseman, A. C. Immunosuppressive Medications, *Clin. J. Am. Soc. Nephrol.* **2016**, *11*, 332-343.

[2] Coutinho, A. E.; Chapman, K. E. The Anti-Inflammatory and Immunosuppressive Effects of Glucocorticoids, Recent Developments and Mechanistic Insights. *Mol. Cell. Endocrinol.* **2011**, *335*, 2–13.

[3] Schreiber, S. L.; Crabtree, G. R. The mechanism of action of cyclosporin A and FK506, *Immunol. Today.* **1992**, *13*, 136-142.

[4] Horby, P.; Lim, W. S.; Emberson, J. R.; Mafham, M.; Bell, J. L.; Linsell, L.; Staplin, N.; Brightling, C.; Ustianowski, A.; Elmahi, E.; Prudon, B.; Green, C.; Felton, T.; Chadwick, D.; Rege, K.; Fegan, C.; Chappell, L. C.; Faust, S. N.; Jaki, T.; Jeffery, K.; Montgomery, A.; Rowan, K.; Juszczak, E.; Baillie, J. K.; Haynes, R.; Landray, M. J. Dexamethasone in Hospitalized Patients with Covid-19. *N. Engl. J. Med.* **2021**, *384*, 693–704.

[5] Gao, D.; Li, T.; Li, X.-D.; Chen, X.; Li, Q.-Z.; Wight-Carter, M.; Chen, Z. J. Activation of Cyclic GMP-AMP Synthase by Self-DNA Causes Autoimmune Diseases. *Proc. Natl. Acad. Sci. U.S.A.* **2015**, *112*, E5699–E5705.

[6] Ahn, J.; Barber, G. N. Self-DNA, STING-dependent signaling and the origins of autoinflammatory disease, *Curr. Opin. Immunol.* **2014**, *31*, 121–126.

[7] Thim-uam, A.; Prabakaran, T.; Tansakul, M.; Makjaroen, J.; Wongkongkathep, P.; Chantaravisoot, N.; Saethang, T.; Leelahavanichkul, A.; Benjachat, T.; Paludan, S.; Pisitkun, T.; Pisitkun, P. STING Mediates Lupus via the Activation of Conventional Dendritic Cell Maturation and Plasmacytoid Dendritic Cell Differentiation. *iScience*, **2020**, *23*, 101530.

[8] Jeremiah, N.; Neven, B.; Gentili, M.; Callebaut, I.; Maschalidi, S.; Stolzenberg, M.-C.; Goudin, N.; Frémond, M.-L.; Nitschke, P.; Molina, T. J.; Blanche, S.; Picard, C.; Rice, G. I.; Crow, Y. J.; Manel, N.; Fischer, A.; Bader-Meunier, B.; Rieux-Laucat, F. Inherited STING-Activating Mutation Underlies a Familial Inflammatory Syndrome with Lupus-Like Manifestations. *J Clin. Invest.* **2014**, *124*, 5516–5520.

[9] Lodi, L.; Melki, I.; Bondet, V.; Seabra, L.; Rice, G. I.; Carter, E.; Lepelley, A.; Martin-Niclós, M. J.; Adba, Al, B.; Bader-Meunier, B.; Barth, M.; Blauwblomme, T.; Bodemer, C.; Boespflug-Tanguy, O.; Dale, R. C.; Desguerre, I.; Ducrocq, C.; Dulieu, F.; Dumaine, C.; Ellul, P.; Hadchouel, A.; Hentgen, V.; Hié, M.; Hully, M.; Jeziorski, E.; Lévy, R.; Mochel, F.; Orcesi, S.; Passemard, S.; Pouletty, M.; Quartier, P.; Renaldo, F.; Seidl, R.; Shetty, J.; Neven, B.; Blanche, S.; Duffy, D.; Crow, Y. J.; Frémond, M.-L. Differential Expression of Interferon-Alpha Protein Provides Clues to Tissue Specificity Across Type I Interferonopathies. *J. Clin. Immunol.* **2021**, *41*, 603–609.

[10] König, N.; Fiehn, C.; Wolf, C.; Schuster, M.; Cura Costa, E.; Tüngler, V.; Alvarez, H. A.; Chara, O.; Engel, K.; Goldbach-Mansky, R.; Günther, C.; Lee-Kirsch, M. A. Familial Chilblain Lupus Due to a Gain-of-Function Mutation in STING. *Ann. Rheum. Dis.* **2017**, *76*, 468–472.

[11] Fuska, J.; Nemec, P.; Kuhr, I. Vermiculine, a new antiprotozoal antibiotic from *Penicillium vermiculatum*. *J. Antibiot.* **1972**, *25*, 208–211.

[12] Jones, D.; Anderson, H. A.; Russell, J. D.; Fraser, A. R. Vermiculine, a metabolic product from *Talaromyces Wortmannii*. *Trans. Br. Mycol. Soc.* **1984**, *83*, 718–721.

[13] Fuska, J.; Ivanitskaya, L.; Horáková, K.; Kuhr, I. The cytotoxic effects of a new antibiotic vermiculine. *J. Antibiot.* **1974**, *27*, 141–142.

[14] Horáková, K.; Kernáčová, B.; Nemec. P.; Fuska, J. Characterization of the cytotoxic activity of vermiculine. *J. Antibiot.* **1976**, *29*, 1109–1111.

[15] Rovenský, J.; Lackovič, V.; Veselková, Z.; Košková, E.; Fuska, J. Vermiculine-induced decrease in cytokine production by human leukocytes. *Int. J. Immunother.* **1997**, *18*, 55–60.

[16] Rovenský, J.; Buc, M.; Blažíčková, S.; Ferenčík, M.; Rauová, L.; Fuska, J.; Stančíková, M. Screening of immunological properties of vermiculine in selected model situations. *Ann. New York Acad. Sci.* **1997**, *815*, 369–371.

[17] Zajícová, A.; Múčková, M.; Krulová, M.; Rychnavská, Z.; Holáň, V. Immunosuppressive effects of vermiculine in vitro and in allotransplantation system in vivo. *Int. Immunopharmacol.* **2001**, *1*, 1939–1945.

[18] Tsakos, M.; Clement, L. L.; Schaffert, E. S.; Olsen, F. N.; Rupiani, S.; Djurhuus, R.; Yu, W.; Jacobsen, K. M.; Villadsen, N. L.; Poulsen, T. B. Total synthesis and biological evaluation of rakicidin a and discovery of a simplified bioactive analogue. *Angew. Chem. Int. Ed.* **2016**, *55*, 1030–1035.

[19] Villadsen, N. L.; Jacobsen, K. M.; Keiding, U. B.; Weibel, E. T.; Christiansen, B.; Vosegaard, T.; Bjerring, M.; Jensen, F.; Johannsen, M.; Tørring, T.; Poulsen, T. B. Synthesis of ent-BE-43547A1 reveals a potent hypoxia-selective anticancer agent and uncovers the biosynthetic origin of the APD-CLD natural products. *Nat. Chem.* **2017**, *9*, 264–272.

[20] Hansen, B. K.; Loveridge, C. J.; Thyssen, S.; Wørmer, G. J.; Nielsen, A. D.; Palmfeldt, J.; Johannsen, M.; Poulsen, T. B. STEFs: Activated vinylogous protein-reactive electrophiles. *Angew. Chem. Int. Ed.* **2019**, *58*, 3533–3537.

[21] Wørmer, G. J.; Hansen, B. K.; Palmfeldt, J.; Poulsen, T. B. A cyclopropene electrophile that targets glutathione s-transferase omega-1 in cells. *Angew. Chem. Int. Ed.* **2019**, *58*, 11918–11922.

[22] Wørmer, G. J.; Villadsen, N. L. Nørby, P.; Poulsen, T. B. Concise asymmetric syntheses of streptazone a and abikoviromycin, *Angew. Chem. Int. Ed.* **2021**, *60*, 10521-10525.
[23] Wu, Z.-C.; Boger, D. The quest for supernatural products: the impact of total synthesis in complex natural products medicinal chemistry, *Nat. Prod. Rep.* **2020**, *37*, 1511-1531.
[24] Itoh, H.; Inoue, M. Comprehensive structure-activity relationship studies of macrocyclic natural products enabled by their total syntheses. *Chem. Rev.* **2019**, *119*, 10002–10031.
[25] Maier, M. E. Design and synthesis of analogues of natural products. *Org. Biomol. Chem.* **2015**, *13*, 5302–5343.
[26] Li, L.; Chen, Z.; Zhang, X.; Jia, Y. Divergent strategy in natural product total synthesis. *Chem. Rev.* **2017**, *117*, 3752–3832.
[27] Szpilman, A. M.; Carreira, E. M. Probing the biology of natural products: molecular editing by diverted total synthesis. *Angew. Chem. Int. Ed.* **2010**, *49*, 9592–9628.
[28] Sun, A. W.; Lackner, S.; Stoltz, B. M. Modularity: Adding New Dimensions to Total Synthesis, *Trends. Chem.* **2008**, *1*, 630–643.
[29] Lehmann, J. W.; Blair, D. J.; Burke, M. D. Towards the generalized iterative synthesis of small molecules, *Nat. Rev. Chem.* **2018**, *2*, 0115.
[30] Li, Q.; Pellegrino, J.; Lee, D. J.; Tran, A. A.; Chaires, H. A.; Wang, R.; Park, J. E.; Ji, K.; Chow, D.; Zhang, N.; Brilot, A. F.; Biel, J. T.; van Zundert, G.; Borrelli, K.; Shinabarger, D.; Wolfe, C.; Murray, B.; Jacobson, M. P.; Mühle, E.; Chesneau, O.; Fraser, J. S.; Seiple, I. B. Synthetic group A streptogramin antibiotics that overcome Vat resistance, *Nature* **2020**, *586*, 145–150.
[31] Lin, S.; Liu, H.; Svenningsen, E. B.; Wollesen, M.; Jacobsen, K. M.; Andersen, F. D.; Moyano-Villameriel, J.; Pedersen, C. N.; Nørby, P.; Tørring, T.; Poulsen, T. B. Expanding the antibacterial selectivity of polyether ionophore antibiotics through diversity-focused semisynthesis, *Nat. Chem.* **2021**, *13*, 47–55.
[32] Karageorgis,G.; Foley, D. J.; Laraia, L.; Brakmann, S.; Waldmann, H. Pseudo natural products—chemical evolution of natural product structure, *Angew. Chem. Int. Ed.* **2021**, doi: 10.1002/anie.202016575.
[33] Foley, D. J.; Zinken, S.; Corkery, D.; Laraia, L.; Pahl, A.; Wu, Y.-W.; Waldmann, H, Phenotyping Reveals Targets of a Pseudo‐Natural‐Product Autophagy Inhibitor, *Angew. Chem. Int. Ed.* **2020**, *59*, 12470-12476.
[34] Morrison, K. C.; Hergenrother, P. J. Natural products as starting points for the synthesis of complex and diverse compounds, *Nat. Prod. Rep.* **2014**, *31*, 6-14.
[35] Llabani, E.; Hicklin, R. W.; Lee, H.-Y.; Motika, S. E.; Crawford, L. A.; Weerapana, E., Hergenrother, P. J. Diverse compounds from pleuromutilin lead to a thioredoxin inhibitor and inducer of ferroptosis, *Nat. Chem.* **2019**, *11*, 521.
[36] Sedmera, P.; Vokoun, J.; Podojil, M.; Vaněk, Z.; Fuska, J.; Nemec, P.; Kuhr, I. Structure of vermiculine, a new nine-membered lactone from *Penicillium vermiculatum*. *Tetrahedron Lett.* **1973**, *14*, 1347–1348.
[37] Boeckman Jr., R. K.; Fayos, J.; Clardy, J. A revised structure of vermiculine. A novel macrolide dilactone antibiotic from *Penicillium vermiculatum*. *J. Am. Chem. Soc.* **1974**, *96*, 5954–5956.
[38] Corey, E. J.; Nicolaou, K. C.; Toru, T. Total synthesis of (±)-vermiculine. *J. Am. Chem. Soc.* **1975**, *97*, 2287–2288.
[39] Seebach, D.; Suering, B.; Kalinowski, H.-O.; Lubosch, W.; Renger, B. Synthesis and determination of the absolute configuration of pyrenophorin and vermiculine. *Angew. Chem. Int. Ed.* **1977**, *16*, 264–265.
[40] Suering, B.; Seebach, D. Synthese und bestimmung der absoluten konfiguration von norpyrenophorin, pyrenophorin and vermiculin. *Liebigs Ann. Chem.* **1978**, 2044–2073.

[41] Fukuyama, Y.; Kirkemo, C. L.; White, J. D. A novel synthesis of (±)-vermiculine. *J. Am. Chem. Soc.* **1977**, *99*, 646–647.

[42] Burri, K. F.; Cardone, R. A.; Chen, W. Y.; Rosen, P. Preparation of macrolides via the Wittig reaction: a total synthsis of (–)-vermiculine. *J. Am. Chem. Soc.* **1978**, *100*, 7069–7071.

[43] Wakamatsu, T.; Yamada, S.; Ban, Y. Synthesis of dl-vermiculine via control of olefin formation. *Heterocycles* **1986**, *24*, 309–312.

[44] Noda, A.; Aoyagi, S.; Michinaga, N.; Kibayashi, C. Total synthesis of (–)-vermiculine. *Tetrahedron Lett.* **1994**, *35*, 8237–8240.

[45] Steip, P.; Breit, B. Concise total synthesis of (–)-vermiculine through a Rhodium-catalyzed C_2-symmetric dimerization strategy. *Chem. Eur. J.* **2019**, *25*, 3532–3535.

[46] Ganss, S.; Breit, B. Enantioselective Rhodium-catalyzed atom-economical macrolactonization. *Angew. Chem. Int. Ed.* **2016**, *55*, 9738–9742.

[47] Steip, P.; Breit, B. Enantioselective Rhodium-catalyzed dimerization of ω-allenyl carboxylic acids: straightforward synthesis of C_2-symmetric macrodiolides. *Angew. Chem. Int. Ed.* **2018**, *57*, 6572–6576.

[48] Sharma, G. V. M.; Mallesham, S.; Mouli, C. C. Studies directed toward the first total synthesis of acremodiol and acremonol. *Tetrahedron: Asymmetry* **2009**, *20*, 2513–2529.

[49] Tsakos, M.; Schaffert, E. S.; Clement, L. L.; Villadsen, N. L.; Poulsen, T. B. Ester coupling reactions – an enduring challenge in the chemical synthesis of bioactive natural products. *Nat. Prod. Rep.* **2015**, *32*, 605–632.

[50] For examples of two-manifold Wacker oxidation on macrodiolides, see e.g.: Barth, R.; Mulzer, J. Two-directional total synthesis of efomycine M and formal total synthesis of elaiolide. *Tetrahedron* **2008**, *64*, 4718–4735.

[51] Nozoe, S.; Hirai, K.; Tsuda, K.; Ishibashi, K.; Shirasaka, M.; Grove, J. F. The structure of pyrenophorin. *Tetrahedron Lett.* **1965**, *6*, 4675–4677.

[52] Motwani, M.; Pesiridis, S.; Fitzgerald, K. A. DNA sensing by the cGAS-STING pathway in health and disease, *Nat. Rev. Genet.* **2019**, *20*, 657-674.

[53] Rehwinkel, J.; Gack, M. U. RIG-I-like receptors: their regulation and roles in RNA sensing, *Nat. Rev. Immunol.* **2020**, *20*, 537-551.

[54] Deerhake, M. E.; Biswas, D. D.; Barclay, W. E.; Shinohara, M. L. Pattern Recognition Receptors in Multiple Sclerosis and Its Animal Models, *Front. Immunol.* **2019**, *10*, 2644

[55] Davidson, S.; Steiner, A.; Harapas, C. R.; Masters, S. L. An Update on Autoinflammatory Diseases: Interferonopathies, *Curr. Rheumatol. Rep.* **2018**, *20*, 38.

[56] Beutler, B. TLR4 as the mammalian endotoxin sensor, *Curr. Top. Microbiol. Immunol.* **2002**, *270*, 109-120.

ToC

10.1002/anie.202105793

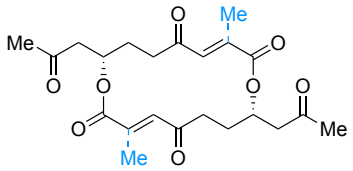

(-)-vermiculine
analogue LH519

- Modular, enantioselective synthetic route to macrodiolides related to vermiculine.
- 18 analogs prepared.
- Analogues identified with cancer cell line selective toxicity.
- LH519 inhibits innate immune signaling pathways, without notable toxicity.

A modular and flexible synthesis of macrodiolides related to the natural product vermiculine is described. The synthesis utilizes a common building block, prepared through a catalytic asymmetric route, to enable various modifications to the scaffold and stereochemical flexibility. Partial blocking of the keto-enoate groups afforded the analogue LH519 which exhibits broad inhibition of innate immune signaling pathways, including cGAS-STING.

@ThomasBPoulsen
@Chemistry_AU
@NatSci_AU